Phi: Jurnal Pendidikan Fisika dan Terapan
Vol. 13, No. 1 (2027) 1-14
ISSN: 2460-4348, e-ISSN: 2549-7162
https://jurnal.ar-raniry.ac.id/index.php/jurnalphi/index

Article Type: *original research*

Identification of Land Subsidence Zone Distribution Using Ground Penetrating Radar Integrated with Cone Penetration Test: A Case Study of Maritime Museum and Syahbandar Tower, North Jakarta

Alya Ayu Triana[1], Rizka Aulia Shakila Rahim[1*], Selvi Misnia Irawati[1], Acep Ruchimat[2]
[1]Geophysical Engineering, Sumatera Institute of Technology, South Lampung, Indonesia
[2]Center for Groundwater and Enviromental Geology, Bandung, Indonesia

Correspondence E-mail: rizkaasr@gmail.com

ARTICLE INFO

Article History:
Received: 26 May 2026
Revised: 25 June 2026
Accepted: 30 July 2026
Published: 09 August 2026

Keywords:
Land Subsidence; Ground penetrating radar; Cone penetration test; Maritime museum; Syahbandar tower

ABSTRACT

Land subsidence is a serious environmental issue in the coastal area of North Jakarta, particularly in Penjaringan District, where the historic buildings of the Maritime Museum and Syahbandar Tower are located. Identification of subsurface conditions regarding the distribution of subsidence zones is necessary to prevent structural damage that could result in significant losses. This study was conducted by integrating Ground Penetrating Radar (GPR) and cone penetration test (CPT). GPR measurements were performed using a GSSI SIR 4000 instrument at a frequency of 400 MHz, with a total of 8 survey lines and 2 CPT points. The radargram results show downward sloping reflections indicating land subsidence beneath the surface. Land subsidence zones were detected at depths of 0 – 3 m at different distances, presumably caused by deformation and uneven compaction. A fill soil layer was detected at depths of 0 – 1.5 m. The correlation between GPR and CPT data confirms the presence of sandy clay with cone tip resistance values of qc = 10–20 kg/cm^2 at depths of 0–4 meters, indicating very low bearing capacity consistent with the land subsidence identified in the GPR data. The results of this method demonstrate that the integration of GPR and CPT data provides a comprehensive and reliable assessment of land subsidence vulnerability as a basis for mitigation planning and sustainable development in the Jakarta area. Accordingly, this study bears significant relevance to the fields of applied physics and geophysics.

This work is licensed under a Creative Commons Attribution-ShareAlike 4.0 International License

1. INTRODUCTION

The current rapid growth in Jakarta is placing increasing pressure on the environment and affecting the quality of life of its residents (Abidin et al., 2015). One of the current environmental issues of serious concern is land subsidence. This condition is supported by data from the latest mapping results, which show that several areas of Jakarta are below sea level (Abidin et al., 2015). In the coastal areas of North Jakarta, the rate of land subsidence continues to increase significantly due to excessive groundwater extraction and the weight of building structures (Marwanza et al., 2023).

Land Subsidence can cause damage to urban insfrastructure, building deformation, and increase the area's vulnerability to flooding and waterlogging (Davydzenka et al., 2024). The average rate of land subsidence in Jakarta's coastal areas using Ground Penetrating Radar (GPR) and InSAR surveys is higher than in other regions, at approximately 3–10 cm/year (Abidin et al., 2015). Based on multi-track InSAR analysis during the period 2017–2022, the land subsidence rate in the coastal area of North Jakarta ranges from 7.44 - 8.47 cm/year and is highly vulnerable to land subsidence due to consolidation of clay layers and groundwater extraction, both from shallow aquifers (< 40 m) and deep aquifers (> 40 m) (Harintaka et al., 2024). InSAR, radar altimetry, and corrected tide gauge analysis consistently identify land subsidence as the primary coastal threat in Jakarta, with a subsidence rate of 60 mm/year that far exceeds the regional sea level rise rate of 3.2 mm/year (Bott et al., 2021). Furthermore, road subsidence along Jakarta's North Coast, as indicated by GPR results and core drilling data, is attributed to the presence of a very soft marine clay layer (Budiono & Noviadi, 2012). This phenomenon of subsidence in Jakarta's coastal areas is consistent with findings from other coastal urban areas worldwide, where land subsidence is frequently concentrated in land reclamation zones, particularly in areas with underground infrastructure and buildings with shallow foundations (Hu et al., 2019).

Land subsidence is a serious issue, especially when it occurs in coastal areas, as these regions are highly vulnerable to environmental pressures from both land and sea. The direct impacts include cracks in houses/buildings, damage and cracks on local roads and highways, as well as damage and tilting of residential buildings that potentially lead to economic losses. The indirect impact of land subsidence is the increasingly widespread expansion of flooding areas (Gumilar et al., 2012). Land subsidence can occur on both a local and regional scales, influenced by several factors (Abidin et al., 2013). First, natural subsidence caused by geological processes such as tectonic activity, geological cycles, and natural consolidation of young alluvial soil. Second, subsidence caused by the weight of structures built on the ground, which leads to compaction or consolidation of the underlying soil layers. Third, subsidence caused by excessive and uncontrolled groundwater extraction.

The rate of land subsidence can be measured using old buildings and historic areas (Rukayah et al., 2025). One of the affected areas in Maritime Museum and Syahbandar Tower in Penjaringan District, North Jakarta. Land subsidence in this area not only impacts the environment and infrastructure but also potentially threatens the preservation of historic buildings. Changes in the proportions of these buildings occurred due to the elevation of surrounding roads and the raising of the building floors to prevent tidal floodwater from entering the museum. The ground floor of the building was raised by approximately 150–200 cm, causing the entrance height to decrease from the original 400–500 cm to 250 cm, and it is now below street level (Rukayah et al., 2025).

In the process of environmental geological mapping to understand the potential hazards of land subsidence, geophysical methods are essential for non-destructively assessing subsurface conditions (Vázquez et al., 2025). The GPR method works based on the principle that electromagnetic wave reflections occur at boundaries between materials with differing dielectric constants and conductivity. GPR survey results indicate that clay layers in coastal areas produce distinctive reflector patterns, namely parallel, continuous, and strong reflectors with high conductivity. These characteristics are highly relevant for identifying land subsidence zones in North Jakarta, which are dominated by soft marine clay layers (Budiono & Latuputty, 2016). Transition zones that are beginning to compact exhibit varying dielectric values depending on the degree of water saturation. Meanwhile, layers undergoing further compaction have lower dielectric values due to reduced water content and porosity (Annan, 2009). These significant differences allow the GPR method to map reflection boundaries and determine the distribution of zones vulnerable to land subsidence (Annan, 2009).

GPR measurements on the coastal road section of North Jakarta show that local geological conditions are the main cause of land subsidence (Budiono & Noviadi, 2012). Nonetheless, no research has yet identified land subsidence zones in Penjaringan area, particulary at Maritime Museum and Syahbandar Tower using GPR geophysical method. Previous research has generally focused on the North Jakarta regional scale or coastal road infrastructure, and there is a lack of integrated studies between geophysics and geotechnical data. Based on this eficiency, this study aims

to identify the distribution of land subsidence prone zone in the Maritime Museum and Syahbandar Tower areas by integrating geophysical method and geotechnical data (CPT), which is expected to provide a more comprehensive interpretation as a basis for mitigation and urban planning. Unlike previous studies that generally used GPR or CPT data separately, the novelty of this study lies in the spatial and depth correlation between GPR radargram reflectors and CPT cone tip resistance (qc) values near the Maritime Museum and Syahbandar Tower. This integrated approach enables more accurate identification of subsurface weak zones, while also providing important insight for the preservation of historic buildings in coastal areas.

2. METHODS

2.1 Research Metodology

This study was conducted at the Maritime Museum and Syahbandar Tower, located in the Penjaringan area of North Jakarta. The geological map of the Jakarta and Kepulauan Seribu (Figure 1) indicates that the area is part of the Mandala Formation, a component of the Bogor sedimentary basin consisting of Tertiary-aged sedimentary rocks and Quaternary volcanic rocks, surface deposits, and intrusive igneous rocks, encompassing the northern Jakarta coastal alluvial plain with topography highly susceptible to subsidence and seawater intrusion. The study area is dominated by the Alluvial Formation (Qa) of clayey sand, silt, and loam formed from river deposits, coastal deposits, and the Ciliwung-Angke swamp, followed by the Coastal Bar Deposits (Qbr) consisting of coarse sandy clasts and mollusk shells dating from the Pleistocene to the Holocene, and the Alluvial Fan Unit (Qav) spreading from young volcanic mountains originating from the Bogor highlands, forming a thick layer with high organic content. The upper soil layers are dominated by soft clay and sandy silt with high compressibility and low bearing capacity, making them highly susceptible to compaction and consolidation (Permana & Rahardjo, 2022).

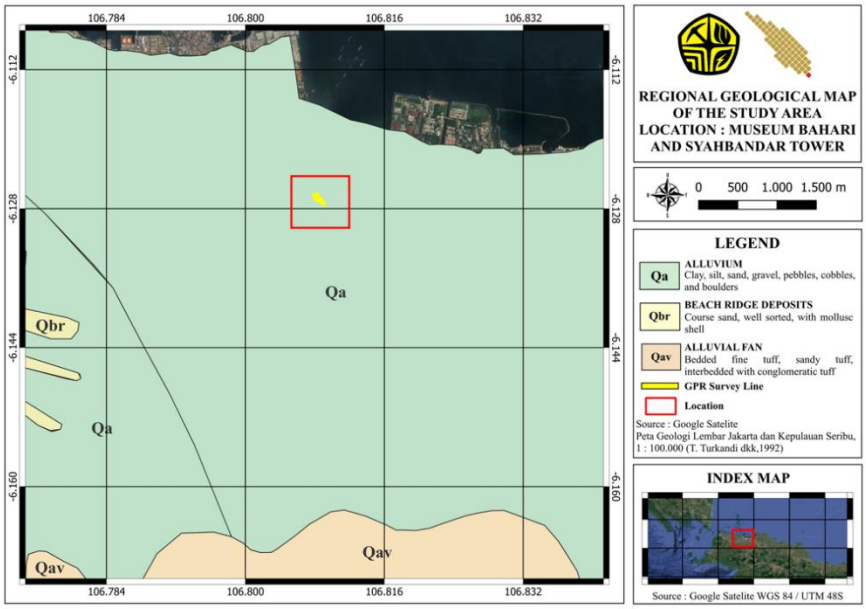


Figure 1. Regional geological map of the study area (T. Turkandi, 1992)

The data used were obtained from measurements conducted by the Center for Groundwater and Environmental Geology (PATGTL) using a GSSI SIR 4000 instrument operating at a frequency of 400 MHz, with a total of 8 survey lines and was supported by data 2 CPT points (Figure 2). GPR data processing was carried out using ReflexW software. The GPR and CPT data obtained were then processed to produce clearer radargrams and vertical cross-sections for interpretation.

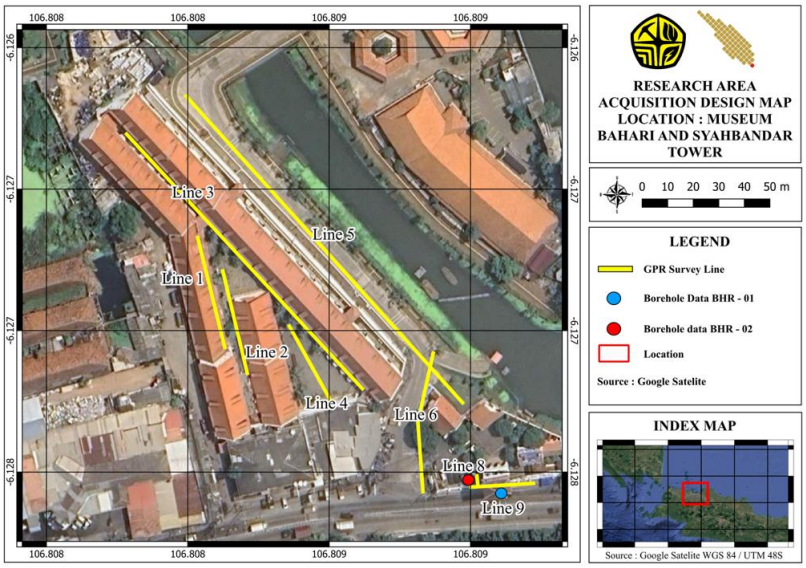


Figure 2. GPR research area acquisition design map

The data processing stages can be briefly seen in the flowchart (Figure 3), began with move starttime, which corrects the initial time point of the reflection signal on each trace, so that the first wave arrival time is reset to 0 ns(Rumansah et al., 2025). This was followed by subtract-mean (dewow), a filter used to remove very low-frequency components (Annan, 2009). Subsequently, DC Shift was applied to shift the signal amplitude values so that the baseline (zero line) is positioned at its true zero (Guo et al., 2023). Automatic gain control (AGC) was then applied to amplify the signal, as electromagnetic waves emitted into the subsurface become increasingly weak with depth due to attenuation (Putri et al., 2025). This was followed by the bandpass butterworth filter, which functions to eliminate extremely high or very low-frequency noise (De Benedetto et al., 2015). Subsequently, background removal was applied to eliminate the effects of additional noise on the signal caused by background interference (Patsia et al., 2023). This was then followed by running average to smooth the signal by averaging several adjacent traces (Rumansah et al., 2025).. Finally, gain was applied again to amplify the signal after the smoothing process carried out in the previous stage (Putri et al., 2025).

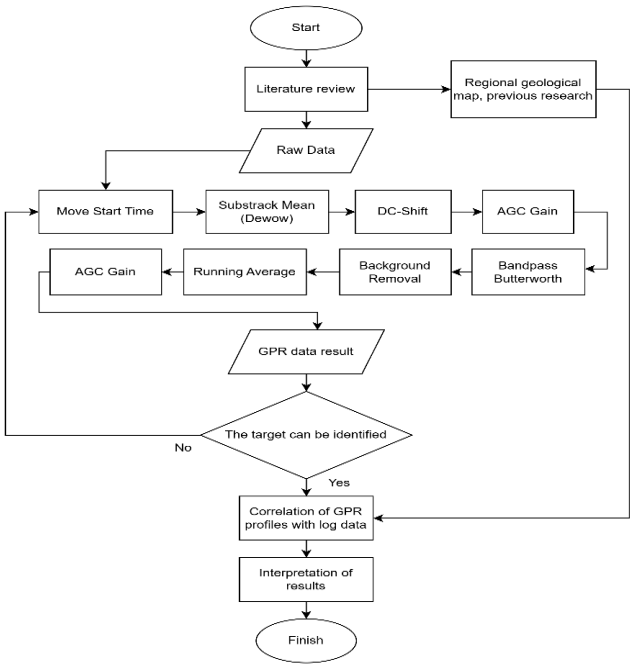


Figure 3. Research metodology flowschart

2.2 Ground Penetrating Radar (GPR)

Ground Penetrating Radar (GPR) is a non-destructive geophysical method that uses high-frequency electromagnetic waves (10 MHz – 2.6 MHz) to detect subsurface anomalies. The principle of this method involves emitting electromagnetic (EM) waves that are reflected by subsurface materials due to differences in their electrical properties (dielectric permittivity) (Annan, 2009). Electromagnetic waves, the fundamental principle of the GPR method, are based on Maxwell's equations, can be written in the following equation :

$$\nabla . D = q \tag{1}$$

$$\nabla . B = 0 \tag{2}$$

$$\nabla \times \vec{E} = -\frac{\partial B}{\partial t} \tag{3}$$

$$\nabla \times H = J + \frac{\partial D}{\partial t} \tag{4}$$

Where D is the electric displacement (C/m^2), B is the magnetic induction or flux density (Tesla), $\vec{E}$ is the electric field intensity (V/m), dan H is the magnetic field intensity (A/m). From Maxwell's equations above, it can be seen that the speed of electromagnetic waves in a medium depends on the speed of light (c = 3.00×10^8 m/s) and the dielectric constant, to determine the depth of the target. can be written in the following equation :

$$\mathrm{v} = \frac{\mathrm{c}}{\sqrt{\varepsilon_r}} \tag{5}$$

The GPR method is influenced by the electromagnetic properties of the subsurface medium, such as relative permittivity, material conductivity, and magnetic permeability. These parameters control the mechanism of electromagnetic wave propagation within a medium. The reflection coefficient (R) is the ratio of reflected energy to incident energy. Its value depends on the physical properties of the medium, particulary the difference in relative dielectric permittivity ($\boldsymbol{\varepsilon_r}$) between layers. Therefore, the reflection coefficient (R) can be written in the following equation :

$$\mathrm{R} = \frac{\sqrt{\varepsilon_2} - \sqrt{\varepsilon_1}}{\sqrt{\varepsilon_2} + \sqrt{\varepsilon_1}} \tag{6}$$

Radar waves propagating through an interface between layers will undergo attenuation due to energy loss during propagation. This energy loss (attenuation) is caused by absorption, which is the conversion of electromagnetic energy into thermal energy. The interaction of the waves with the medium's electrical and magnetic properties determines the magnitude of this attenuation. The rate of decrease in wave amplitude is expressed as attenuation (α), which depends on the physical and electromagnetic properties of the medium and can be written in the following equation :

$$\alpha = \omega\sqrt{\frac{\mu\varepsilon}{2}}\left[\left(\left(1 + \frac{\sigma^2}{\omega^2\varepsilon^2}\right)^{\frac{1}{2}} - 1\right)^{\frac{1}{2}}\right] \tag{7}$$

$$\delta \approx \frac{\sigma}{2}\sqrt{\frac{\sigma}{\varepsilon}} \; untuk\; \sigma \ll \omega\varepsilon \tag{8}$$

Where α is the attenuation coefficient (dB/m) depends on the magnetic permeability (μ) (H/m), ε is the permittivity (F/m) , σ is the conductivity (mS/m).

Skin depth indicates the maximum depth to which an electromagnetic wave can penetrate a medium before its amplitude is attenuated to approximately 37% or 1/e of its initial amplitude. The

higher the frequency, the smaller the skin depth, resulting in shallower penetration but higher resolution. Conversely, high conductivity accelerates wave attenuation and shortens the skin depth. Therefore, in media with high conductivity, low frequencies are used to achieve deeper penetration. Therefore, to achieve optimal penetration depth, especially in areas with high conductivity, such as wet soil and highly conductive rock, it is necessary to use lower frequencies. Skin depth can be written in the following equation :

$$\delta \approx 0{,}0053 \frac{\sqrt{\varepsilon_r}}{\sigma} \; untuk \; \sigma \ll \omega\varepsilon \tag{9}$$

Where δ is the skin depth (m), σ is the conductivity (s/m), f is the frequency (Hz), and ε_r is the dielectric constant or relative permittivity.

2.3 Cone Penetration Test (CPT)

Cone penetration test (CPT) is a soil resistance testing tool used to examine in-situ bearing capacity and total shear strength per tested depth (Permana & Rahardjo, 2022). The test is conducted by pressing the cone-shaped tip of the sondir, known as the cone, into the soil at a rate of 1–2 cm/s (penetration) to a depth of 5 cm, after which the cone resistance value is recorded as the cone tip is pushed an additional 5 cm deeper so that the side of the cone also moves (Yu et al., 2022). The total resistance (q_1) is higher in sand than in clay of the same strength, and the ratio of The total resistance (q_1) and sleeve friction (q_s) is lower in sand than clay (Zwara & Bałachowski, 2022).

$$R_f = \frac{Sleeve\ friction}{Cone\ tip\ resistance} \; x\ 100\ \% \tag{10}$$

Where the friction ratio R_f represents the correlation factor between the cone tip resistance reading and the sleeve friction, which is the ratio of the cross-sectional area of the cone to the surface area of the cone sleeve, total resistance (q_1) and cone tip resistance (q_t) (Cho et al., 2023). Furthermore, the ratio of sleeve friction (q_s) to cone tip resistance (q_t) can be calculated as the friction ratio (R_f). The magnitude of the friction ratio (R_f) plays an important role in estimating the type of soil layer. Coarse-grained soils (sand) will have a lower friction ratio (R_f) value compared to fine-grained soils (clay and silt). The Cone Penetration Test (CPT) is important for soil classification and foundation design. Furthermore, it is widely employed in the estimation of pile foundation bearing capacity (Sližytė et al., 2024).

3. RESULT AND DISCUSSION

3.1 Ground Penetrating Radar *(GPR)* Analysis

The results from Line 1 (Figure 4a) indicate the presence of a newly filled layer at a depth 0 – 1.2 meters, consistent with direct field observations at the Maritime Museum (Figure 4c), where the ground floor level is almost level with the bottom of the windows due to land subsidence and recurring tidal flooding (rob flood)(Rukayah et al., 2025). In the area marked by the red box, a weakening of the signal amplitude can be observed indicating the boundary between the fill layer and the underlying layer. In the area marked by the red box, a weakening of signal amplitude can be observed, indicating the boundary between the fill layer and the underlying layer. This reflection occurs due to the dielectric permittivity contrast between the two layers, while the amplitude attenuation is caused by the high water content and fine-grained materials in the alluvial soil, which increase both conductivity and permittivity, thereby enhancing GPR signal attenuation (Budiono & Noviadi, 2012). The salinization effects as shown (Figure 4b), identified as a high-salinity zone, indicates the occurrence of seawater intrusion and previous tidal flooding, and suggests the potential for continuous soil compaction(Giambastani et al., 2020). The signal amplitude becomes stronger again in the zone identified as the old ground surface, which represents an older and denser layer beneath the fill material.

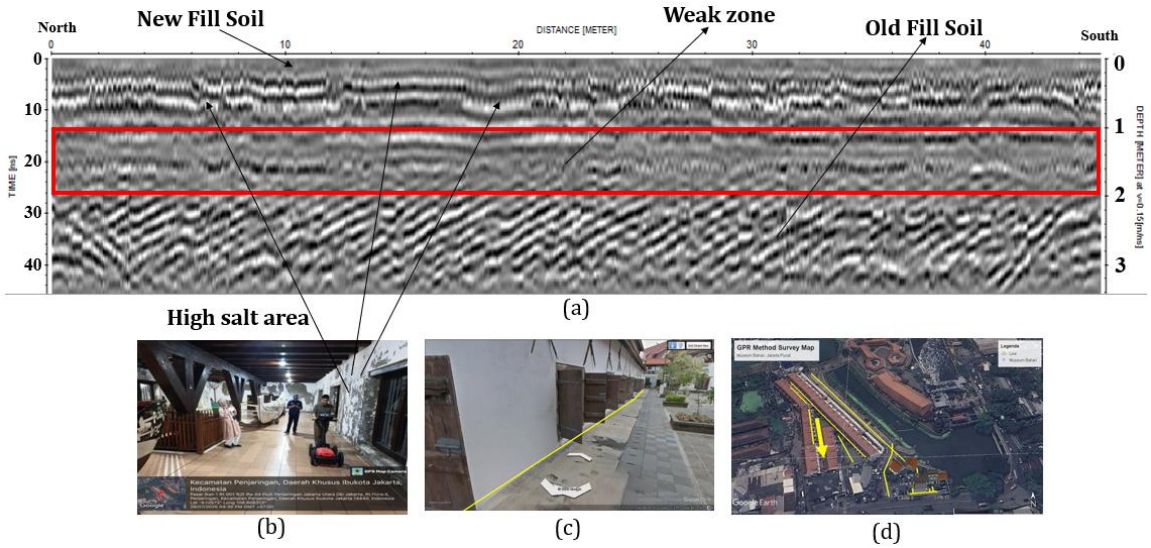


Figure 4. (a) GPR radargram interpretation result of line 1. (b) Salinization effects on building wall. (c) Field condition along the survey path during data acquisition. (d) GPR survey path and line direction.

The results of Line 2 (Figure 5a), the zones marked with yellow lines at depths of 1 m and 3 m indicate ground subsidence caused by excessive loading from the structures above, as well as the soft and compressible nature of the alluvial soil. This is further supported by field conditions (Figure 5b), where the ground floor level has been elevated, similar to Line 1. Structural loading on alluvial clay soils accelerates consolidation, which contributes to regional land subsidence and indicating the settlement observed in this area represents a local example of the broader subsidence process occurring along the Jakarta coastal zone (Widiarso et al., 2019). The consolidation process in this water saturated soil increases the dielectric permittivity and reduces the propagation velocity of the electromagnetic wave. The weak zone marked by the red box also shows a weakening of the GPR signal due to the high permittivity and conductivity of the water saturated material, which increases the potential for subsidence.

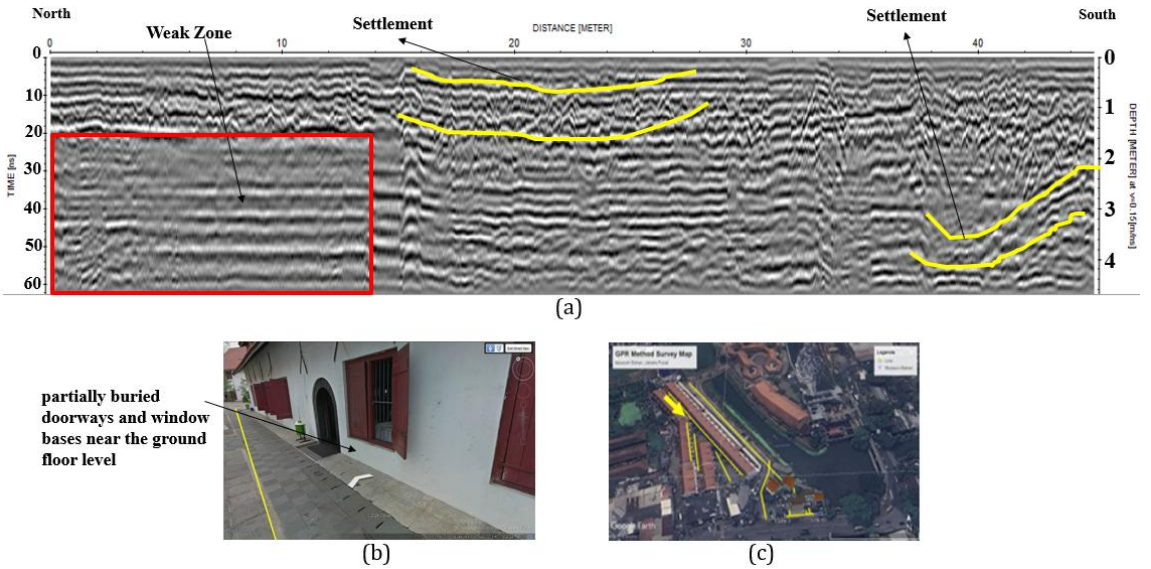


Figure 5. (a) GPR radargram interpretation result of line 2. (b) Field condition along the survey path during data acquisition. (c) GPR survey path and line direction.

The results of Line 3 (Figure 6a), show that zone marked by the yellow line represents a layer experiencing land subsidence at a depth of 1 m. The weak zone marked by the red box at a depth of 2 – 3 m shows amplitude weakening and chaotic reflections, interpreted as water-saturated alluvial

material with high permittivity and conductivity that increase signal attenuation. This is supported by field conditions (Figure 6c) which show that the building floor has undergone elevation, as indicated by the lower part of the window frames being nearly level with the newly elevated ground floor (Pandapotan, 2023). The signal amplitude strengthens again with increasing depth, indicating the presence of a denser layer with lower dielectric permittivity, consistent with the local geological conditions characterized by sandy alluvium.

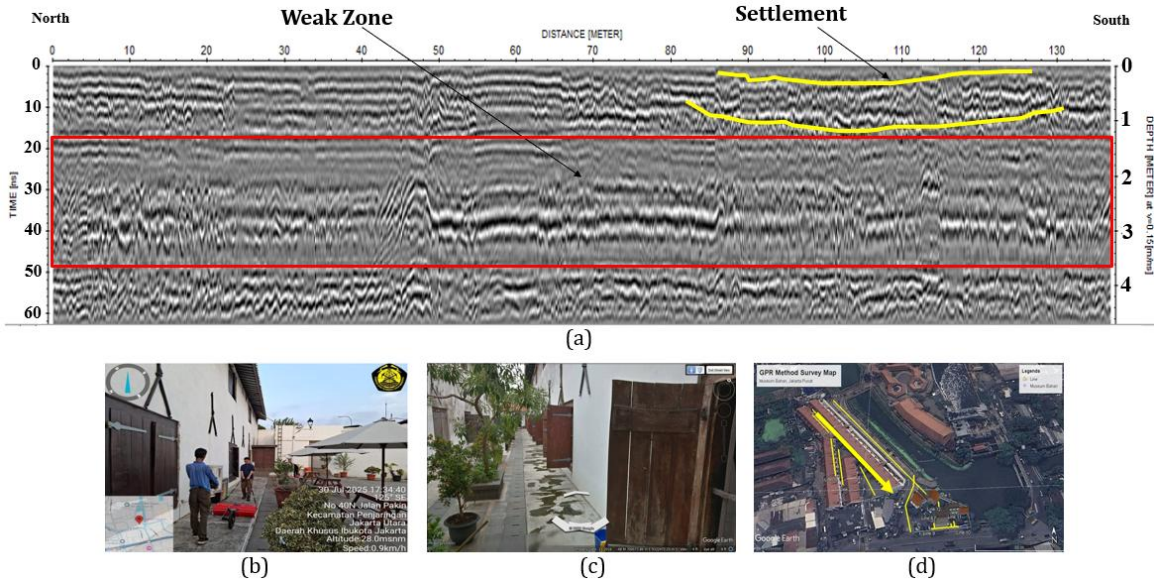


Figure 6. (a) GPR radargram interpretation of line 3. (b) and (c) Field condition along the survey path during data acquisition. (d) GPR survey path and line direction.

Based on the results of Line 4 (Figure 7a) show that the yellow line indicates a settlement zone at a depth of 1–2 m, characterized by a downward-sloping reflection pattern, presumably indicating land subsidence caused by the soft and compressible nature of the alluvial soil. A weak zone identified on the radargram at a depth of 2–4 m is marked by amplitude attenuation, which may be caused by water-saturated alluvial material with high permittivity and conductivity that increases signal attenuation.

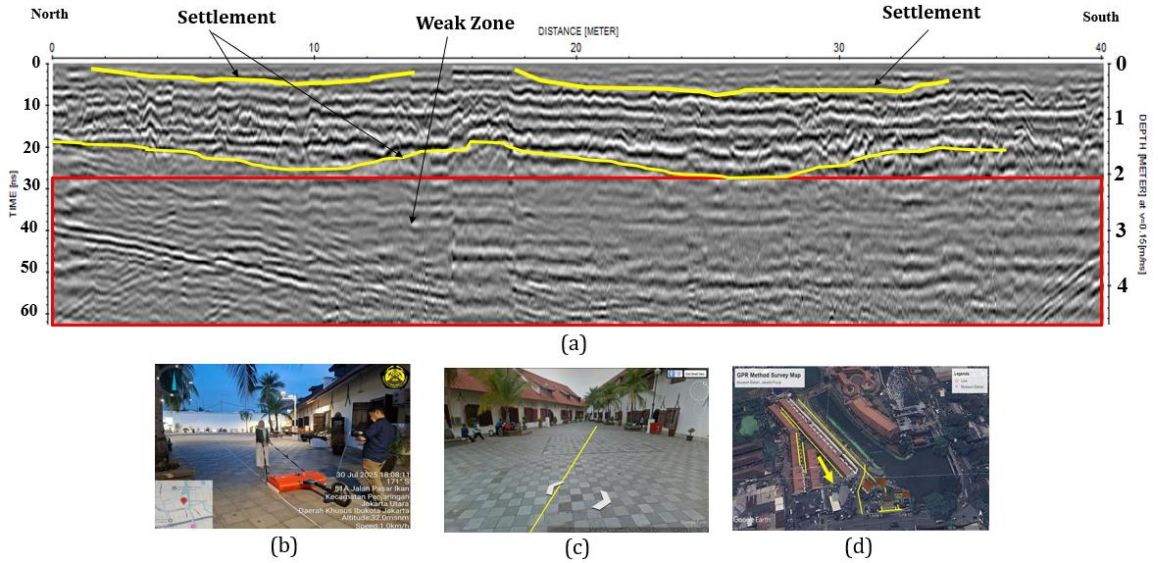


Figure 7. (a) GPR radargram interpretation of line 4. (b) and (c) Field condition along the survey path during data acquisition. (d) GPR survey path and line direction.

Based on the results of Profile 5 (Figure 8a), the zones marked with yellow lines at a depth of 1 m exhibits land subsidence, indicated by a downward sloping reflection pattern in the radargram. The weakening of signal amplitude at a depth of 1.5 m is interpreted as the boundary between the fill layer and the old ground surface. This is presumably caused by alluvial soil conditions that increase electrical conductivity and result in GPR signal attenuation. Subsequently, the signal amplitude strengthens again, indicating the presence of an older and denser layer. This indication of land subsidence is further supported by field observations (Figure 8c), such as the Maritime Museum area appearing lower than its surroundings.

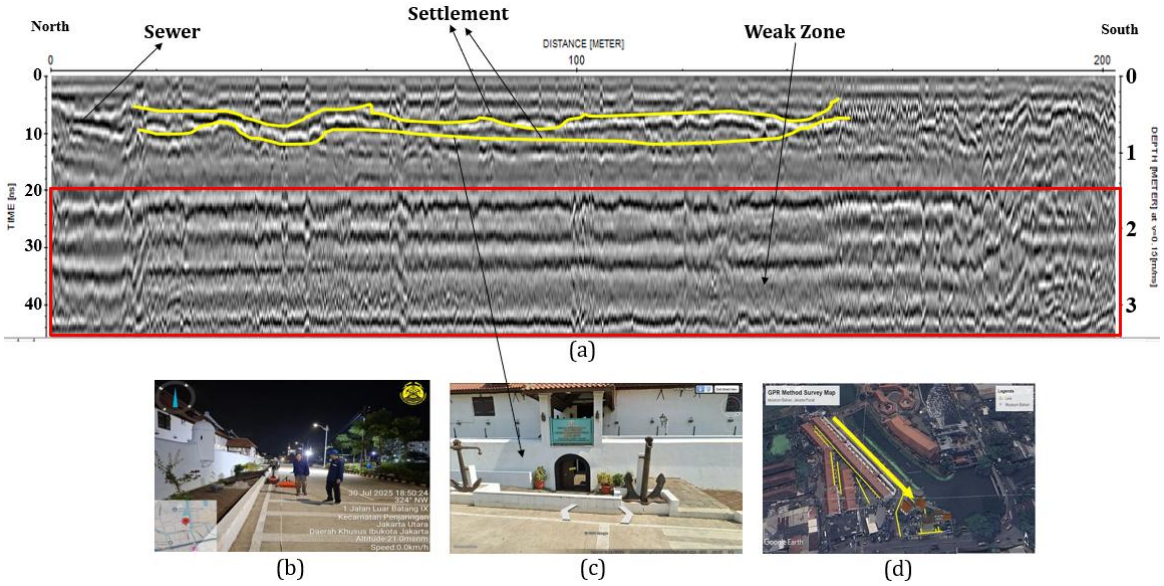


Figure 8. (a) GPR radargram interpretation of line 5. (b) and (c) Field condition along the survey path during data acquisition. (d) GPR survey line and line direction.

Based on the results of Profile 6 (Figure 9a), at a depth of 1 m along the survey line at distances of 6–50 m, a decrease in the ground surface is indicated by a yellow line showing a relatively downward-sloping reflection pattern, indicating lateral variations in both layer thickness and material properties, such as changes in moisture content or density. The zone marked by the red box at a depth of 2–3 m exhibits amplitude weakening, presumably due to subsurface structural disturbances or higher moisture content and permittivity, which can be interpreted as a weak zone.

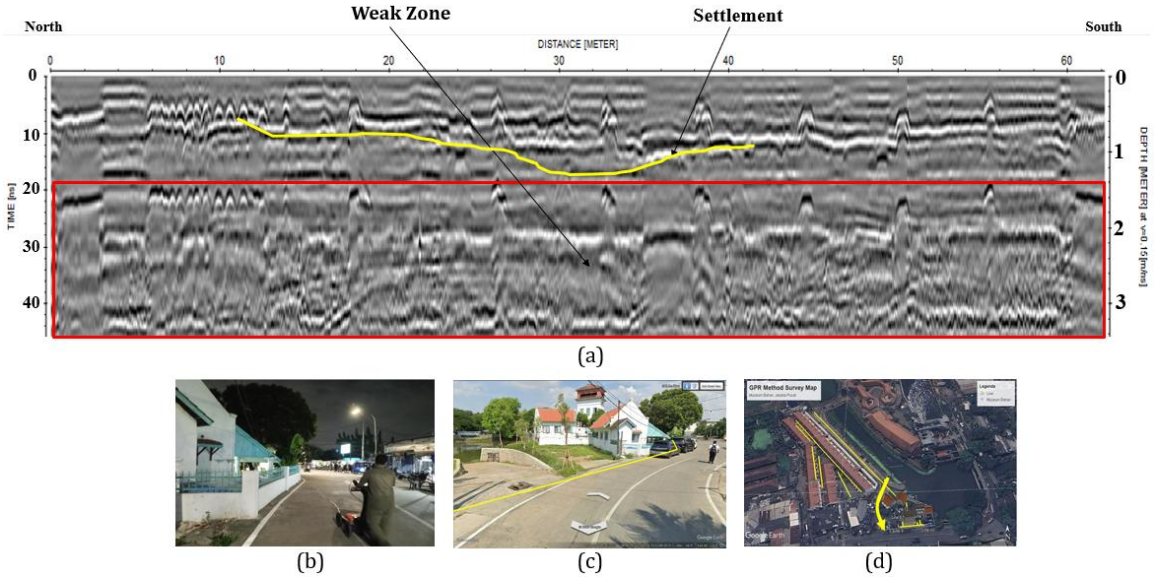


Figure 9. (a) GPR radargram interpretation of line 6. (b) and (c) Field condition along the survey path during data acquisition. (d) GPR survey path and line direction

Based on the results of profile 8 (Figure 10a), the zones marked with yellow lines at depths of 1–2 and 4 meters show a gradual decrease in reflectivity toward the south, this pattern indicates a change in the geometry of the layers, which are no longer horizontal, caused by the soft nature of the alluvial soil. A zone with low amplitude, identified at depths of 1.5–3.6 meters, indicates high attenuation, likely associated with conductive materials such as water-saturated clay (Ghazali et al., 2025). Media with high clay content, moisture levels, and permittivity cause greater attenuation of electromagnetics waves, resulting in lower GPR signal amplitudes compared to sandier media(Svendsen et al., 2023). This increases the potential for ground subsidence and has caused a 6.5-degree tilt in the Syahbandar Tower, as shown in Figure 9b.

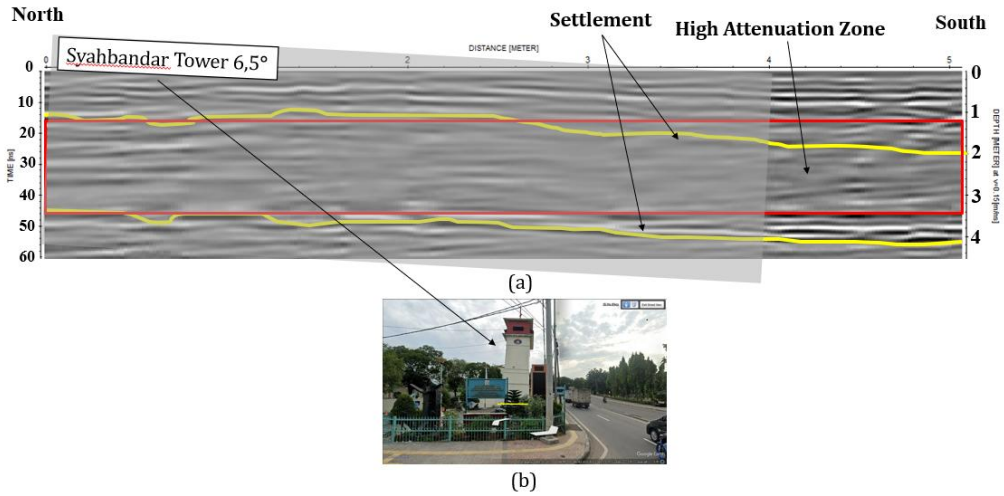


Figure 10. (a) GPR radargram interpretation of line 8. (b) Field condition along the survey path during data acquisition.

Based on the results of profile 9 (Figure 11a) the radargram shows the presence of a relatively homogeneous overburden layer at a depth of 0–1 meter. Then, at a depth of approximately 1.5–2.5 meters, there is a strong reflector marking a lithological boundary, with a chaotic pattern below it that likely represents material fragmentation in a zone of high heterogeneity. This zone is potentially associated with deformation resulting from uneven compaction, and the tendency for changes in the reflector's geometry indicates the onset of subsurface deformation. Indications of land subsidence are also supported by field observations (Figure 10c), such as the Syahbandar Tower area, which appears to be tilted 6.5 degrees toward the south (Rukayah et al., 2025).

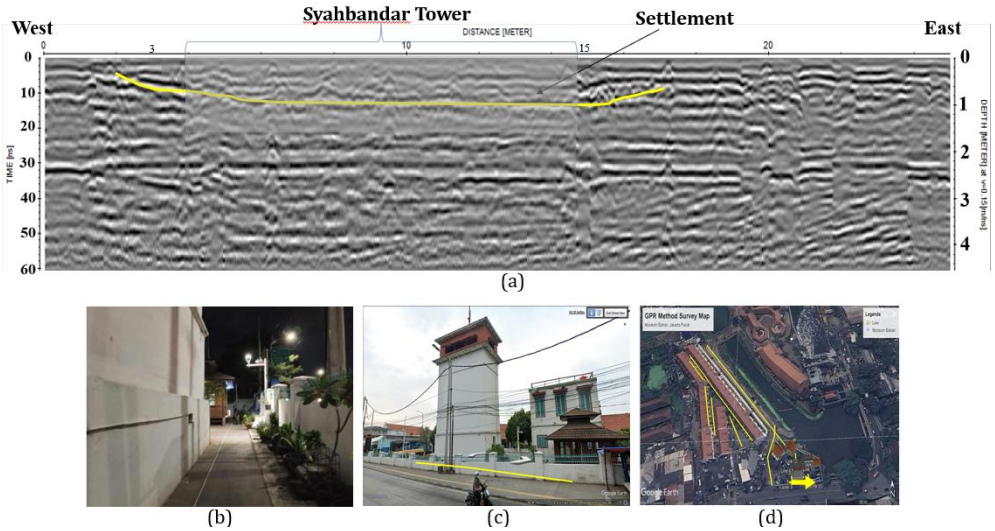


Figure 11. (a) GPR radargram interpretation of line 9. (b) and (c) Field condition along the survey path during data acquisition. (d) GPR survey path and line direction.

3.2 Correlation of GPR Data with Sondir test

The test data were obtained from PT. Delta Arsitektur Persada in a cultural consultation presentation regarding the conservation planning of the Syahbandar Tower. The sondir equipment used has a capacity of 2.5 tons and was conducted on the eastern side of the Syahbandar Tower building. The test was carried out until reaching the equipment capacity with the value $q_c \geq 150$ kg/cm^2 is presented in Table 1.

Table 1. Sondir Test Result of Syahbandar Tower (source : Maritime Museum of Jakarta)

Depth (m)	Value of q_c (kg/cm^2)	*Soil type*
0 – 4	10 – 20	Sandy clay (sand mixed with clay)
4 – 10	15 – 30	Sandy clay (sand mixed with clay)
10 – 14	8 – 10	Sandy clay (sand mixed with clay)
14 – 28	10 - 25	Sandy clay (sand mixed with clay)
≥ 28	≥ 20	Sandy clay (sand mixed with clay)

The sondir test data of Syahbandar Tower is correlated with the GPR records from Line 8 and Line 9 (Figure 12 and 13) due to the proximity of the sondir test point location. This correlation aims to integrate the geophysical parameters from GPR data with the geotechnical parameters from the sondir test. Although the cone penetration test data in Table 2 are available to depths exceeding 28 m, the correlation between the GPR data and the cone penetration test data in this study uses only data from depths of 0-4 m. This due to the limited penetration depth of the GPR, meaning that only this layer can be directly compared with the CPT data.

On Line 8 (Figure 12a), the reflection pattern that slopes downward toward the south supports the actual condition of the Syahbandar Tower, which has a tilt of approximately 6.5°. This gradual subsidence is related to uneven soil compaction beneath the structure. This is supported by the results of the cone penetration test in Table 3, which indicate that the soil layers at the Syahbandar Tower site are dominated by sandy clay at all tested depths. At depths of 0–4 m, the tip resistance (qc) values range only from 10–20 kg/cm^2, indicating a very weak surface layer that is easily deformed, thereby allowing differential settlement to occur, which causes the building to tilt.

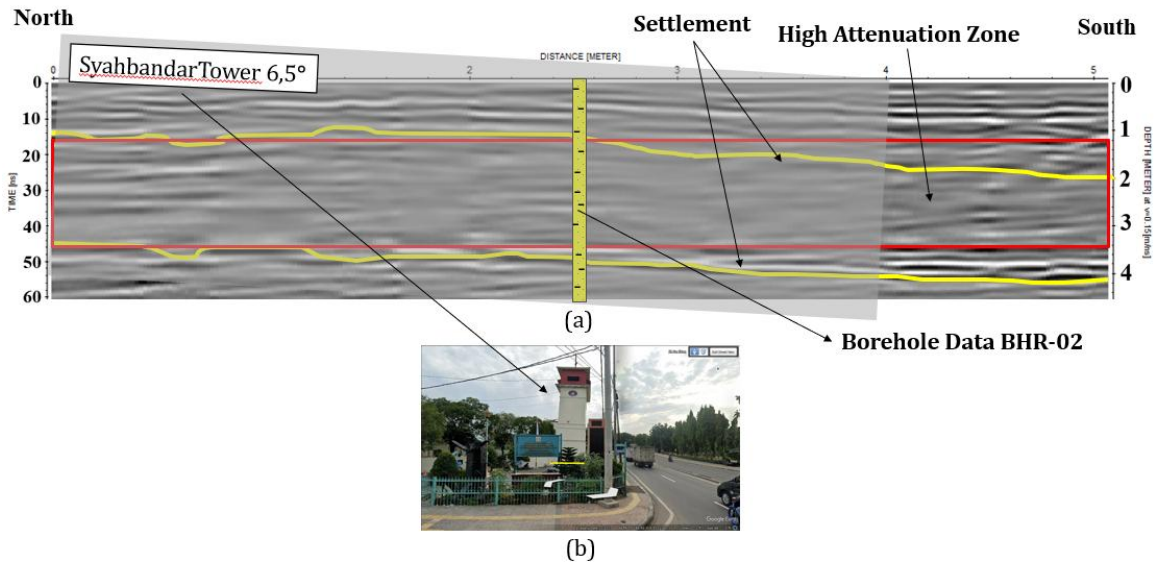


Figure 12. (a) Correlation Line 8 with sondir test BHR – 02. (b) Field condition along the survey path during data acquisition

Meanwhile, Profile 9 (Figure 13a) indicates the presence of an overburden layer at a depth of 0–1 meter and a zone of high heterogeneity beneath it, a finding supported by the results of the cone penetration test in Table 3, where at depths of 0–4 m, the qc value is only 10–20 kg/cm^2, indicating that the uppermost layer consists of material with low bearing capacity that is highly susceptible to external disturbances and changes in environmental conditions. This heterogeneous zone may be related to variations in moisture content, changes in material composition, or layer deformation due to building loads. These conditions align with the characteristics of sandy clay in the cone penetration test data, which exhibits highly variable properties when saturated with water and subjected to continuous pressure.

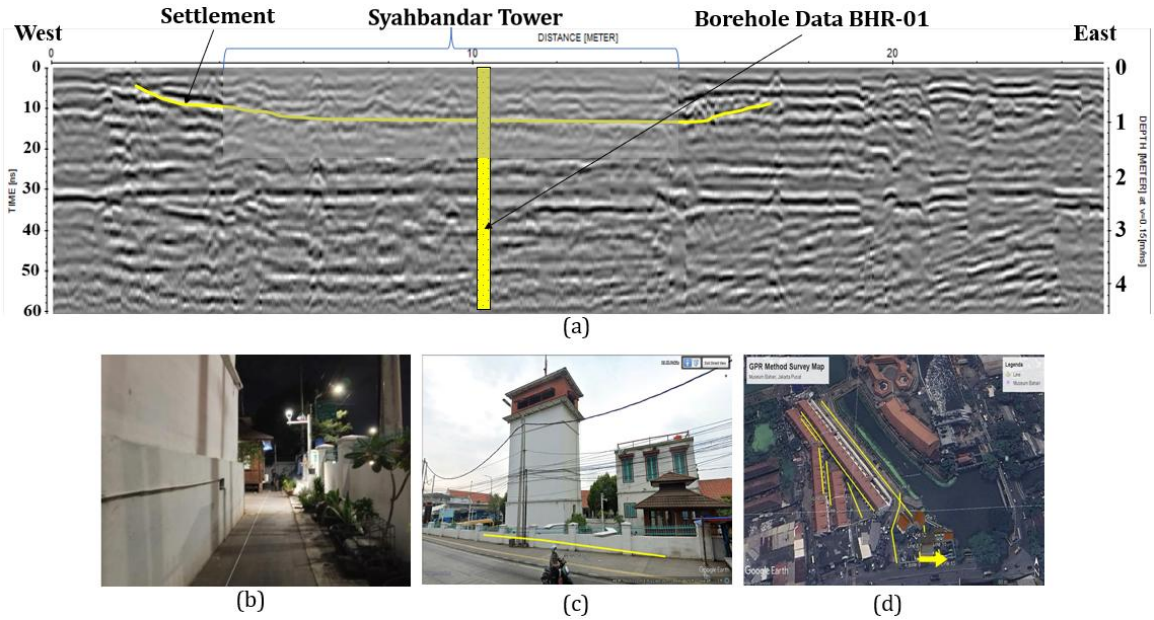


Figure 13. (a) Correlation Line 9 with sondir test BHR – 01. (b) and (c) Field condition along the survey path during data acquisition. (d) GPR survey path and line direction

The capability of GPR to detect subsurface anomalies is governed by the dielectric permittivity of the subsurface materials. In the Penjaringan area, the soft alluvial soil layers exhibit high water saturation, in which water possesses a dielectric constant of approximately 80, resulting in the absorption of GPR electromagnetic energy and subsequent signal attenuation at shallow depths (Tronics & Bahder, 2019). This interpretation is further supported by the CPT results, which reveal very low cone resistance (qc) values at corresponding depths, thereby confirming the presence of weak and water-saturated sediments. The correlation between GPR signal attenuation and low qc values indicates that the dielectric properties of the soil directly reflect its geotechnical conditions.

4. CONCLUSION

Based on the results of this study, it can be concluded that on Lines 1 – 5 located in the Maritime Museum area, layers susceptible to land subsidence were detected at depths of 0 – 1.5 m, with additional weak zones extending to depths of 2 – 3 m in several profiles, caused by the soft and compressible nature of the alluvial soil combined with surface loading from the overlying building structures. Based on result from Lines 6 – 9 located in the Syahbandar Tower area, subsurface structural disturbances were indicated at depths of 1 – 3 m, associated with deformation, uneven compaction, and the presence of voids, which accelerate the consolidation process and increase the potential for land subsidence.

The integration of GPR data with sondir (CPT) results at the Syahbandar Tower successfully validates the interpreted subsurface conditions. Cone tip resistance values (qc = 10 – 20 kg/cm^2) at depths of 0 – 4 m confirm the presence of sandy clay with very low bearing capacity, consistent with the weak zones identified in GPR Lines 8 and 9. The downward sloping reflection pattern in Line 8

further corroborates the observed 6.5° tilt of the Syahbandar Tower, attributed to land subsidence beneath the building structure. This integration demonstrates that combining GPR and CPT data provides a more comprehensive and reliable assessment of land subsidence vulnerability compared to either method applied independently, as GPR utilizes physical parameters such as wave propagation velocity and electromagnetics wave attenuation to detect dielectric contrasts between soil layers, whereas CPT directly measures bearing capacity through the cone tip resistance values (qc), so that the two methods complement each other in identifying weak zones susceptible to land subsidence but alsoo makes a tangible contribution to applied physics as an efficient framework for non-destructive urban geotechnical surveys, while also serving as a case study in educational training for shallow exploration geophysics.

ACKNOWLEDGEMENTS

We would like to express sincere gratitude to Center for Groundwater and Environmental Geology (Pusat Air Tanah & Geologi Tata Lingkungan) for providing the opportunity and facilities to conduct this research. Special thanks are also extended to the author's parents and friend for their continuous support, prayers and motivation during completion of this study.

REFERENCES

Abidin, H. Z., Andreas, H., Gumilar, I., & Brinkman, J. J. (2015). Study on the risk and impacts of land subsidence in Jakarta. *Proceedings of the International Association of Hydrological Sciences*, *372*, 115–120. https://doi.org/10.5194/piahs-372-115-2015

Abidin, H. Z., Andreas, H., Gumilar, I., Sidiq, T. P., & Fukuda, Y. (2013). Land Subsidence in Coastal City of Semarang (Indonesia): Characteristics , Impacts and Causes. *Natural Hazards and Risk, 4(3), 226-240*, *5705*. https://doi.org/10.1080/19475705.2012.692336

Annan, A. P. (2009). Electromagnetic principles of ground penetrating radar. In H. M. Jol (Ed.). In H. M. Jol (Ed.), *Ground Penetrating Radar Theory and Applications* (pp. 3–40). Elsevier. https://doi.org/10.1016/B978-0-444-53348-7.00016-8

Bott, L. M., Schöne, T., Illigner, J., Haghshenas Haghighi, M., Gisevius, K., & Braun, B. (2021). Land subsidence in Jakarta and Semarang Bay – The relationship between physical processes, risk perception, and household adaptation. *Ocean and Coastal Management*, *211*, Article 105775. https://doi.org/10.1016/j.ocecoaman.2021.105775

Budiono, K., & Latuputty, G. (2016). Subsurface Geological Condition of Several Land Coastal Zone in Indonesia Based on the Gssi Ground Probing Radar (Gpr) Record Interpretation. *Bulletin of the Marine Geology*, *23*(1), 9. https://doi.org/10.32693/bomg.23.1.2008.6

Budiono, K., & Noviadi, Y. (2012). Investigation of Ground Penetrating Radar for Detection of Road Subsidence Northcoast of Jakarta, Indonesia. *Bulletin of the Marine Geology*, *27*(2), 87. https://doi.org/10.32693/bomg.27.2.2012.48

Cho, S., Kim, H. S., & Kim, H. (2023). Locally Specified CPT Soil Classification Based on Machine Learning Techniques. *Sustainability (Switzerland)*, *15*(4). https://doi.org/10.3390/su15042914

Davydzenka, T., Tahmasebi, P., & Shokri, N. (2024). Unveiling the Global Extent of Land Subsidence: The Sinking Crisis. *Geophysical Research Letters*, *51*(4), 1–11. https://doi.org/10.1029/2023GL104497

De Benedetto, D., Quarto, R., Castrignanò, A., & Palumbo, D. A. (2015). Impact of Data Processing and Antenna Frequency on Spatial Structure Modelling of GPR Data. *Sensors (Switzerland)*, *15*(7), 16430–16447. https://doi.org/10.3390/s150716430

Ghazali, M. D., Saputra, H., Islam, S. N., & Johari, J. (2025). Revealing the untold stories of sinkhole land subsidence over the remains of an underground river in tuff soil by Ground Penetrating Radar. *Geomatica*, *77*(2), 100078. https://doi.org/10.1016/j.geomat.2025.100078

Giambastani, B. M. S., Macciocca, V. R., Molducci, M., & Antonelli, M. (2020). Factors Affecting Water Drainage Long-Time Series in the Salinized Low-Lying Coastal Area of Ravenna (Italy). *Water*, *12*(256), 1–23. https://doi.org/10.3390/w12010256

Gumilar, I., Abidin, H. Z., Andreas, H., & Sidiq, T. P. (2012). On Mapping and Evaluating the Impacts of

Land Subsidence in Bandung Basin (Indonesia). *FIG Working Week 2012: Knowing to Manage the Territory, Protect the Environment, Evaluate the Cultural Heritage*, *May 2012*, 1–18.

Guo, Y., Liu, G., Jing, G., Qu, J., Wang, S., & Qiang, W. (2023). Ballast fouling inspection and quantification with ground penetrating radar (GPR). *International Journal of Rail Transportation*, *11*(2), 151–168. https://doi.org/10.1080/23248378.2022.2064346

Harintaka, H., Suhadha, A. G., Syetiawan, A., Ardha, M., & Rarasati, A. (2024). Current land subsidence in Jakarta: a multi-track SBAS InSAR analysis during 2017–2022 using C-band SAR data. *Geocarto International*, *39*(1). https://doi.org/10.1080/10106049.2024.2364726

Hu, B., Chen, J., & Zhang, X. (2019). Monitoring the land subsidence area in a coastal urban area with InSAR and GNSS. *Sensors (Switzerland)*, *19*(14), 1–19. https://doi.org/10.3390/s19143181

Marwanza, I., Anugrahadi, A., Sumotarto, U., Kurniawati, R., Yudha, H. F., & Nugraheni, R. D. (2023). Land Subsidence and Geotechnical Impact of Jakarta Kota Area. *Indonesian Journal of Urban and Environmental Technology*, *6*(2), 145–164. https://doi.org/10.25105/urbanenvirotech.v6i2.13981

Patsia, O., Giannopoulos, A., & Giannakis, I. (2023). Background Removal, Velocity Estimation, and Reverse-Time Migration: A Complete GPR Processing Pipeline Based on Machine Learning. *IEEE Transactions on Geoscience and Remote Sensing*, *61*, 1. https://doi.org/10.1109/TGRS.2023.3300276

Permana, A. M., & Rahardjo, P. P. (2022). The site characterization of central jakarta soft soil using CPTu and laboratory test. *Indonesian Geotechnical Journal*, *1*(1), 25–40. https://doi.org/10.56144/igj.v1i1.6

Putri, S. N., Ismail, N., Khatimah, H., & Umar, M. (2025). Use of GPR and ERT Methods to Image Shallow Structures around a Prospective Paleotsunami Geopark Cave in Aceh Besar, Indonesia. *IOP Conference Series: Earth and Environmental Science*, *1479*(1). https://doi.org/10.1088/1755-1315/1479/1/012016

Rukayah, R. S., Tarigan, A. P. M., Marthanty, D. R., Ontowirjo, B., Shofie, A. M. T., & Giovano, F. A. (2025). An extreme land subsidence in North Jakarta from a heritage architecture view. *Journal of Asian Architecture and Building Engineering*, *00*(00), 1–17. https://doi.org/10.1080/13467581.2025.2533217

Rumansah, R. P. P., Paembonan, A. Y., & Andika, P. P. (2025). Pengembangan Aplikasi "Itera-Vision-Gpr-Ui (Itera Vision System for Gpr Utilities Inference)" Berbasis Computer Vision Dengan Model Yolov12 Untuk Deteksi Utilitas Pada Metode Ground Penetrating Radar. *Journal Online of Physics*, *11*(1), 120–131. https://doi.org/10.22437/jop.v11i1.49883

Sližytė, D., Šalna, R., & Urbonas, K. (2024). Statistical Evaluation of Sleeve Friction to Cone Resistance Ratio in Coarse-Grained Soils. *Buildings*, *14*(3). https://doi.org/10.3390/buildings14030745

Svendsen, E. B., Nielsen, L., Nilsson, B., Kjær, K. H., & Looms, M. C. (2023). Crosshole Ground-Penetrating Radar in Clay-Rich Quaternary Deposits: Toward Characterization of High-Loss Media. *Journal of Geophysical Research: Solid Earth*, *128*(5). https://doi.org/10.1029/2022JB025909

Vázquez, R., Carreón-Freyre, D., López, N., Ferrer, V., & Balderas, S. (2025). Assessment of The Origin of New Superficial Deformed Zones Integrating GPR-UAV Surveys and Geological Data, At The NW-Side of Querétaro City, Mexico. *Earth Systems and Environment*. https://doi.org/10.1007/s41748-025-00877-8

Widiarso, D. A., Haryanto, W., Muslim, D., Zakaria, Z., & Iskandarsyah, T. Y. (2019). Potential consolidation settlement due to load stresses of building structures. *International Journal of GEOMATE*, *17*(60), 204–210. https://doi.org/10.21660/2019.60.73924

T. Turkandi, S. D. (1992). Geologic map of Jakarta and Kepulauan Seribu Quadrangles, Jawa. Bandung: Geological Reaserch and Develoment Centre.

Yu, X., Liu, S., & Pei, H. (2022). Design of Cone Penetration Test Data Relay Transmission by Magnetic Communication. *Sensors*, *22*(13). https://doi.org/10.3390/s22134777

Zwara, Ł., & Bałachowski, L. (2022). Prediction of Pile Shaft Capacity in Tension Based on Some Direct CPT Methods—Vistula Marshland Test Site. *Materials*, *15*(7). https://doi.org/10.3390/ma15072426